

Integration of Nanofabrication and Design Optimization: Structure Characterization, Intelligent Modeling, and Performance Evaluation of Phenol Sensor

Chandra P. Sekhar¹, Muhittin Yilmaz², Sajid Bashir¹ and Jingbo Liu^{1*}

1: Chemistry, Texas A&M University-Kingsville, MSC161, 700 Univ. Blvd. Kingsville, TX

2: Electrical Engineering and Computer Science, Texas A&M University-Kingsville, MSC 192, 700 Univ. Blvd. Kingsville, TX

ABSTRACT: A macrosensor incorporating nano components towards detection of phenol compounds was optimized using two intelligent design models and fabricated as a Gibbs-gold hybrid phenol sensor using a sol-gel spin-coating technique to prepare a trapping and detecting elements (Gibbs reagent) to measure phenol concentrations. The limit of detection, sensitivity and response time were determined colorimetrically with superior results to current designs.

Keywords: Phenol sensor, Nanofabrication, Intelligent modeling, Sensor performance

I. INTRODUCTION

Phenol is an organic molecule commonly used to produce various organic compounds and polymers [1] and it can be released into environment from production of phenolic resins [2]. It is widely used in the automotive, construction, plywood, and appliance industries [3] and released to air and water [4-6]. Most methods of analysis require collecting and transporting the samples for further processing [7]. Applications of sensors because of their size and portability have been more successful for field testing of analytes than the lengthy laboratory testing [8]. Sensors may be in the form of microchips, electrodes or thin films [9]. The associated performance degradation in fabrication efficiency and parameter can be avoided by using intelligent models such as artificial neural networks (ANN) [10] and fuzzy logic (FL) [11]. ANN [12] and FL [13] systems integrate the human brain inference logic into their mathematical structures and utilize a black-box approach to explain a system input-output relationship, yielding intelligent models. The FL modeling uses fuzzy sets for the input and output variables and minimizes the corresponding mapping error by adjusting the membership functions. The mathematical structures obtained by using a training data set are also validated by using a test data set, as demonstrated in various applications [14-20].

A. Gibbs Reagent as Sensing Element

Di-halogen substituted quinine-chloroimides (Gibbs' reagent) form stable complexes on interaction with phenol [21]. Interaction of Gibbs reagent with 2- and 6-positions phenol analogues yields a colored complex [22-23].

B. Use of Gold as the Trapping Element

Nanoparticles can be synthesized with ease in solution and the sensing can be operated at ambient temperature. Such advantages with reasonable detection capability caused interests in gold nanoparticles (GNPs) sensors. Properties of gold like chemical inertness and resistance to surface oxidation make GNPs important for use in nanotechnology based devices [24-25]. GNPs show wide variation of optical and dielectric properties in surrounding media due to surface plasma resonance (SPR) [26-27] enables construction of simple, but sensitive colorimetric sensors [28-29].

C. Sol Gel Method to Fabricate Micro Sensor

Sol-gel derived thin films composed of detecting agents like Gibbs has been extensively investigated in colorimetric studies interaction of phenol with Gibbs reagent [30].

D. Neural Networks for Design Optimization

ANNs models can provide powerful input-output mapping capabilities through parallel mathematical interconnections, feed-forward or recurrent networks, mathematical processing elements. These processes mimic neurons, with

transfer functions such as sigmoidal functions or purely linear functions, and training algorithms such as back-propagation are used in different fields. The feed-forward ANN structure with 's' neurons at the hidden layer, is suitable for arbitrary function approximation and contains the model inputs (b_1, \dots, b_r), the model output (z), the input-hidden layers weight coefficients ($w_{ij}; i=1, \dots, r, j=1, \dots, s$), the hidden-output layers weight coefficients ($v_i; i=1, \dots, s$), the bias terms for each hidden neuron (d_i) and the output neuron (k), and the transfer functions $s(\cdot)$. Based on the ANN interconnection, each hidden neuron output ($n_i, i=1, \dots, s$) can be written as

$$n_i = s([b_1 \mathbf{L} b_r] \begin{bmatrix} w_{1i} \\ \mathbf{M} \\ w_{ri} \end{bmatrix} + d_i), \quad i = 1, \mathbf{K}, s \quad (1)$$

Then, the output of the ANN feed-forward structure is obtained as

$$z = s\left(\sum_{i=1}^s v_i \times n_i\right) + k \quad (2)$$

The ANN model weight and bias coefficients are determined by training the initial model. The optimal coefficients yield a minimum modeling error between the ANN model and the a-prior known input-output data. Finally, the trained ANN model is tested by using a new set of input-output data and verifying the acceptable ANN model error.

E. FL and ANFIS for Sensor Optimization

Fuzzy logic uses intuitive natural reasoning to represent systems in terms of black box approach. Fuzzy set and logic theories define system variables vaguely and use degree of membership values for each system input and output, whose interrelated dynamics are stated by using fuzzy inference rules. There are two main inference types; 1) Mamdani type uses a fuzzy output membership function and determines the actual output via inference rules and aggregation algorithms; 2) Sugeno-Takagi type represents the system outputs in terms of constants or linear combinations of the input variables. Any input-output data can be mapped to a black-box fuzzy system via adaptive

algorithms such as adaptive neuro-fuzzy inference system (ANFIS).

The ANFIS [31] develops a fuzzy system model for a system in terms of fuzzy membership sets and inference rules, and error minimization algorithms, i.e., the neural network back-propagation algorithm with or without a least squares algorithm, by using a limited number of time-domain data. The adaptive algorithm is especially useful when there is no prior information about the input-output dynamics or the corresponding membership functions. The fuzzy system model is then tested via a new set of input-output data to validate the model. The ANFIS implementation in Matlab software [32] is mainly limited to Sugeno-Takagi type, multi-input single-output systems.

II. METHOD

A. Fabrication of Sensor

The phenol sensor was constructed by dissolving different concentrations of Gibbs reagent in methanol. This solution was heated and mixed continuously with a magnetic stirrer for 30 minutes in a water bath, then cooled to room temperature. Gum Arabica was added (2 mass %) to improve the uniformity of the film and to control the particle size of the sensing elements. This sol-gel precursor was heated at 60 and 80°C for 2 hrs to evaporate the solvent. Different concentrations of gold chloride trihydrate and ascorbic acid were added in the ratio of 1:1.5 to produce (16 formulations) GNPs to extend the range of the sensor.

B. Nanocharacterization of Sensor

Advanced microscopic analysis help to study analyzing composition, distribution of the sensing agent, and GNPs structure. A field emission scanning electron microscopy (SEM, JSM-6701F, JEOL) was used to determine the sensor thickness and surface morphology. A transmission electron microscopy (TEM) (TEM, Tecnai G2 F20 FEI) was used to determine the fine structure of the sensor. Atomic Force Microscopy (AFM, Nanoscope III, Veeco Cooperation) with tapping mode was

used to determine the topography, particle size and 3D surface image of the sensor.

C. Evaluation of Sensor Performance

In order to evaluate the gold Gibbs hybrid (GGH) sensor performance, a colorimetric study was undertaken to determine the detection limit, response time, and sensitivity for sensor. Formation of the indophenols was the key principle for the colorimetric studies. Studies were conducted in a ceramic watching plate with 12 wells with the surface area of approximately 3.14 cm^2 . Various volumes and concentration of Gibbs reagent and phenol buffer were added to observe the color changes. At time intervals of 15 minutes, a photograph was collected with computer assisted camera and whole experiment was conducted over 24h.

D. Use of ANN and FI Frameworks

The intelligent modeling via ANN and ANFIS was initiated by determining three inputs and one output. To obtain the relative optical density, 16 parameters were used, including concentration of Gibbs ($0.025\text{-}0.25 \mu\text{M}$), GNPs ($0.01\text{-}0.04 \text{ mol/L}$) and phenol ($6\text{-}50 \text{ Vol } \%$). Fabrication and characterization results generate the training and validation input-output data set for the intelligent models.

III. RESULTS AND DISCUSSION

A. Nanostructural Study

SEM images (Fig. 1a-d) depict spherical shape of GGH and a size of about 30-40 nm. GNP's (Fig. 1a) form spherical aggregates and several wide clusters, whose uniformity increases with electrical activity and reaction of Gibbs with phenol. Fig. 1b exhibits the linear cylindrical nature of Gibbs coated with the GNPs and it forms mesh like network. The cross-sectional SEM images of the sol-sensor (Fig. 1c) allow thickness determination to be *ca.* 500 nm. Fig. 1d represents topical surface of the sensor. With the addition of phenol to the GGH sensor, dissolution of porous nature was seen with the formation of the indophenol and loss of mesh work was characterized. TEM images depict the structural morphology with high spatial resolution of the film. Fig. 2a and 2b depicts the

size of spherical GNP's of 30-40 nm. GNP's were agglomerating and possess SPR.

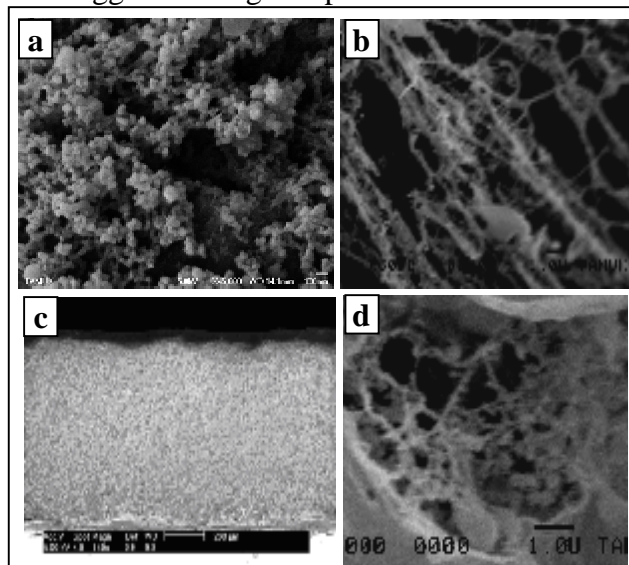


Fig. 1a-d. SEM images of Gibbs and GGH complex

TEM images of GGH depict linear and cylindrical nature of Gibbs reagent with uniform GNP coating. Linear nature of the polymer synthesized in sol method of sensor fabrication possess better sensitivity for the detection of phenol because large area of contact for electron exchange and indophenol complex formation. Loss of network structure of GNP's was observed and this change is consistent with SEM characterization.

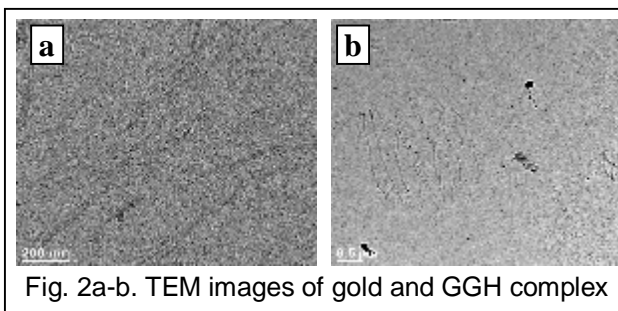


Fig. 2a-b. TEM images of gold and GGH complex

AFM Images depicted the surface morphology and measured the size of the GNP's. Fig. 3a showed the sparse distribution of the GNPs and Fig. 3b the topography of active surface at nano range. Size of GNP's in this study was measured as *ca.* 30-40 nm. The GNPs were coated on the surface of Gibbs. Since AFM studies the top surface layer of sensor film, it depicts the actual layer which is in contact with phenol but it cannot reveal the inner

composition and build up of sensor. GNPs were measured to have an effective diameter of 12 nm for Au, and polydispersity (*polyd*) of 0.267 for the coated particles. Analysis shows the mean particle size of GGH was 485 nm and the distribution of particles (*polyd* of 0.05), being consistent with the SEM findings.

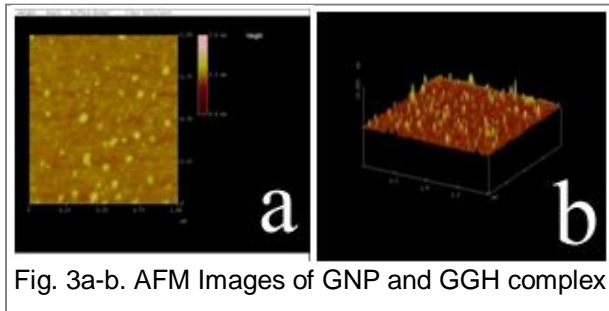


Fig. 3a-b. AFM Images of GNP and GGH complex

B. Sensor Performance

Colorimetric evaluation of the phenol sensor with a concentration of 0.05 mol of Gibbs reagent was studied and color changes of different concentrations of phenol and Gibbs reagent in different dilutions at different intervals of time was captured (data not shown). Initial color was developed within 1h and changes in intensity of color were different with the passage of time. The maximum optical density was calculated to be 255 using the formula,

$$\text{Optical density} = \text{Log}_{10} \left(\frac{255-p}{255-x} \right),$$

where 'p' stands for average back ground correction of well plate (where 'x' stands for mean intensity of well and measurements were recorded as relative optical density): Relative optical density = 1/optical density.

Relative optical density (ROD) of the 12 wells at various intervals was calculated based upon the intensity of color development. Serial numbers from 1 to 12 were the wells and 13 to 16 were the measurements taken for back ground correction and average back ground were calculated.

C. Intelligent Modeling and Validation

The intelligent models by using the neural network and fuzzy logic frameworks aimed to have black-box models, relating the three sensor inputs, and one sensor output. The actual amounts of the input variables were used during

the simulations. The ROD output was obtained from 16 input parameters. 13 data points were used to train the intelligent models and other 3 data points were used to verify the intelligent model prediction performances (Fig. 4).

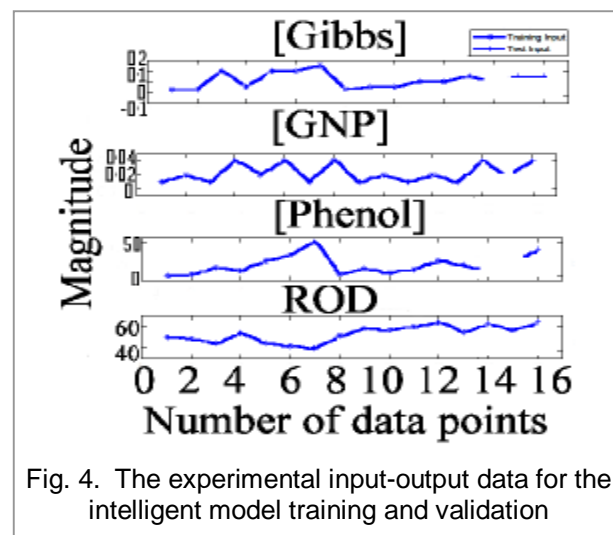


Fig. 4. The experimental input-output data for the intelligent model training and validation

The Matlab Neural Network Toolbox [33] is used to obtain a neural network model approximation for the sensor ROD. A feed-forward network with one hidden layer was created by using 'newff' command. The 'init' command properly initialized the weight coefficients based on the input parameter space. Then, the 'train' command achieves the neural network structure with the optimal weight coefficients.

The corresponding neuron transfer functions and the number of neurons were determined after a number of trials. The optimal combination yielding the best approximation and prediction power was found to be 'tansig' transfer functions for the hidden layer neurons, a 'purelin' transfer function for the output layer neuron, and 12 neurons for the hidden layer via the 'nntool' command and its 'Import' and 'View' options, where the input-to-hidden layer weight coefficients (IW{1,1}), the hidden layer neuron bias terms (b{1}), the hidden layer to output weight coefficients (LW{2,1}), and the output layer neuron bias term (b{2}) were calculated. The neural network approximation based prediction was in line with ROD. It was observed that different number of neurons and transfer functions yielded very different phenol

sensor optical density behavior, especially during the model validation stage.

The Matlab Fuzzy Logic Toolbox [33] was used to obtain an ANFIS approximation for the same phenol sensor ROD data. The ANFIS model was trained by using the 'anfis' command. A number of trials yielded the optimal fuzzy system structure with 4 membership functions on the Gibbs concentration input path while 2 membership functions on the other two input paths, the 'gbellmf' type membership functions for all inputs, 16 fuzzy inference rules, and 16 membership functions for the output, via 'plotfis' command, and via 'anfisedit', 'Generate FIS', 'Structure' commands.

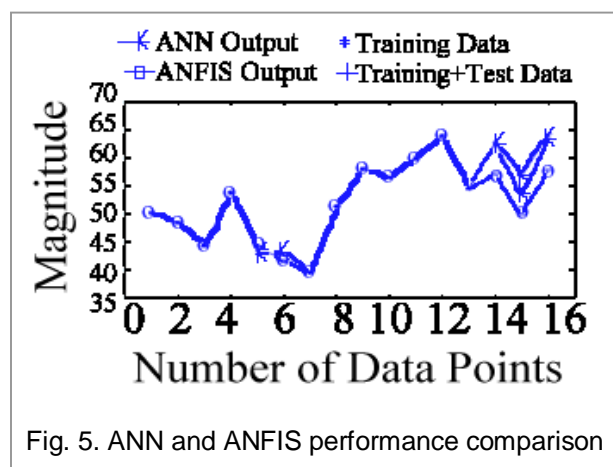


Fig. 5. ANN and ANFIS performance comparison

The corresponding ANFIS approximation and prediction performances indicate that the ANFIS model approximation was perfect while the ANFIS model prediction could only follow the typical behavior of the phenol sensor relative optical value with some non-negligible errors. Different number of membership functions and various membership function types in ANFIS training generated very distinct phenol sensor relative optical values, implying a need for more rigorous training with enhanced and more experimental data. Also, observing the ANFIS training error minimization behavior helped to decide the most appropriate membership functions for the fuzzy system.

The ANN and ANFIS model approximation and prediction performances were also compared

(Fig. 5). Although the training data approximations for both models were almost the same, the prediction performance of the ANN model outperformed the prediction of the ANFIS model. Since these two models have different parameters to adjust for the best prediction, it suggests that both intelligent models have promising potentials to characterize the phenol sensor behavior.

IV. CONCLUSION

A GGH sensor was successfully optimized using ANN and FL models for the colorimetric detection of phenol. The detector was utilizing trapping/detecting elements and derived from SG method. Characterization revealed the nanostructure of the Au-GGH complex as spherical shaped GNPs with size range of 30-40 nm, which was fabricated as linear cylindrical polymers of Gibbs reagents coated with clusters of GNPs. Colorimetric studies were used to test the performance of the sensor. The results indicate that the intermediate color once formed is stable at least for two weeks (the length of the study) at room temperature with a limit of detection of 0.1 μ , sensitivity (36 % ROD) and a fast response time of (< 1 sec) were measured through colorimetric method.

V. ACKNOWLEDGEMENTS

TAMUK, the College of Arts and Sciences Research and Development Fund, (160310-00014) and Robert A. Welch Departmental Grant (AC-0006) are duly acknowledged for funding. The NSF-MRI acquisition and facility access to Microscope and Imaging Center and Materials Characterization Facility at TAMU-College Station are also acknowledged.

VI. REFERENCES

- [1] S. Akai and Y. Kita, **Organic Preparations and Procedures International**, 30, 1998, pp. 603-605.
- [2] Encyclopedia of Polymer Science and Technology - V. 11 "Polymer fibers to Rayon" H.F. Mark, N.G. Gaylord and N.M. Bikales (eds.), pp. 64-69. John Wiley & Sons, Inc, New York, 1969.

- [3] X. Zhang, A. Li, Z. Jiang, Q. Zhang, **Journal of Hazardous Materials**, 137, 2006, pp.1115-1122.
- [4] P.R. Gogate, **Ultrasonics Sonochemistry**, 15, 2008, pp. 1-15.
- [5] J.L. Gerberding, "Properties of Phenol", **U.S Department of Health and Human Services (USDHHS)**, 2002, pp. 1-348.
- [6] P. Martus, W. Puttmann, **The Science of the Total Environment**, 307, 2003, pp. 19-33.
- [7] M.C. Weinberg, G.F. Neilson, "Phase Transformation in Gels", **Sol-Gel Technology For Thin Films, Fibers, Performs, Electronics and Specialty Shapes**, 1st edition, L.C. Klein, (ed.), pp. 28-45. Noyes Publications, Berkshire, 1988.
- [8] E. R. Lowe, C.E. Banks, R.G. Compton, **Analytical Bioanalytical Chemistry**, 383, 2005, pp. 523-531.
- [9] Y. Yu, S. Liu, H. Ju, **Biosensors and Bioelectronics**, 19, 2003, pp. 509-514.
- [10] S. Haykin, **Neural Networks and Learning Machines**, 3rd Ed., pp. 122-230, Prentice-Hall, New York.,2008.
- [11] L.A. Zadeh, **Information and Control**, 8, 1965, pp 338-353.
- [12] G.L. Gerstein, "Assembly, Connectivity and Activity: Methods, Results, Interpretations " **Analysis and Modeling of Neural Systems**, 1st edition, F.H. Eeckman (ed), pp. 3-14, Kluwer Academic Publishers, MA. 2007.
- [13] L.A. Zadeh, **IEEE Transactions on Systems, Man, and Cybernetics**, 3, 1973, pp. 28-44.
- [14] B.D. Ripley "Unsupervised Methods", **Pattern Recognition and Neural Networks**, 1st edition, pp. 286-326, Cambridge University Press, London, 2008.
- [15] Y. Zhang, Z. Tan, K. Chen, Z. Yang, X. Lv, **Robotics & Autonomous Systems**, 57, 2009, pp. 645-651.
- [16] X. Liang, H. Zhang, J. Xiao, Y. Chen, **Neurocomputing**, 72, 2009, pp. 3055-3065.
- [17] M. Yilmaz, "Intelligent Control System Design", **Intelligent Control Approach to Damage-Mitigation Concept**", MSc. Thesis, pp. 48-73. Pennsylvania State University, University Park, PA, 1996.
- [18] H.W. Raybin, **Journal of the American Chemical Society**, 67, 1945, pp. 1621-1623.
- [19] H.D. Gibbs, **Journal of Biological Chemistry**, 81, 1926, pp. 455-455.
- [20] H.D. Gibbs, **Journal of Physical Chemistry**, 31, 1927, pp. 1053-1081.
- [21] J.C. Dacre, **Analytical Chemistry**, 43, 1971, pp. 589-591.
- [22] Y.J. Kim, S.M. Cho, H-B Pyo, C. A. Choi, **Sensors**, 6, 2005, pp. 845-848.
- [23] N. Nath, A. Chilkoti, **Analytical Chemistry**, 74 , 2002, pp. 504–509.
- [24] L.M. Liz-Marzan, **Materials Today**, 7 2004, pp. 26-31.
- [25] G.L. Hornyak, C.J. Patrissi, E.B. Oberhauser, C.R. Martin, J-C Valmalette, L. Lemaire, J. Dutta and H. Hofmann, **Nanostructure Material** ,9, 1997, pp. 571–574.
- [26] J. Liu, Y. Lu, **Journal of Fluorescence**, 14 , 2004, pp. 343-345.
- [27] A.S.Dorcheh, M.H. Abbasi, **Journal of Materials Processing Technology**, 199, 2008, pp. 10-26.
- [28] C Smyth, K. T. Lau, R. L. Shepherd, D. Diamond, Y. Wu, G. M. Spinks and G.G. Wallace, **Sensors and Actuators B: Chemical**, 129 , 2008, pp. 518-524.
- [29] H. Frumkin, J.L. Gerberding," Health risk associated with Phenol," USDHHS, 2008, pp. 1-190.
- [30] A. Lante, A. Crapisi , P. Krastanov , A. Spettoli, **Biochemistry**, 36, 2000, pp. 51-58.
- [31]J.S.R. Jang, **IEEE Transactions on Systems, Man, and Cybernetics**, 23, 1993, pp. 665-685.
- [32] Fuzzy Logic Toolbox, Mathworks, Inc. Natick, MA.
- [33] Neural Network Toolbox, Mathworks, Inc., Natick, MA.